Lithos 282–283 (2017) 215–227

Contents lists available at ScienceDirect

Lithos

journal homepage: www.elsevier.com/locate/lithos

Cenozoic basalts in SE China: Chalcophile element geochemistry, sulfide saturation history, and source heterogeneity

Xiao-Wen Huang [a], Ben-Xun Su [b], Mei-Fu Zhou [c,*], Jian-Feng Gao [a], Liang Qi [a,d]

[a] State Key Laboratory of Ore Deposit Geochemistry, Institute of Geochemistry, Chinese Academy of Sciences, Guiyang 550081, China
[b] State Key Laboratory of Lithospheric Evolution, Institute of Geology and Geophysics, Chinese Academy of Sciences, Beijing 100029, China
[c] Department of Earth Sciences, The University of Hong Kong, Hong Kong, China
[d] State Key Laboratory of Continental Dynamics, Department of Geology, Northwest University, Xi'an 710069, China

ARTICLE INFO

Article history:
Received 24 August 2016
Accepted 18 March 2017
Available online 24 March 2017

Keywords:
Platinum-group element (PGE)
Sulfur-saturation
Heterogeneous mantle source
Cenozoic basalt
SE China

ABSTRACT

Cenozoic basalts in SE China may be derived from a mixture of depleted MORB mantle (DMM) and enriched mantle 2 (EM2) sources, but whether these basalts share a common mantle source or magmatic history remains unknown. To investigate these unresolved issues, this study sampled basalts from Niutoushan and Mingxi (Fujian province), Xilong (Zhejiang province), and Penghu (Taiwan) for geochemical analysis. The basalt samples show OIB-like trace element patterns and have low PGE contents, with 0.02–0.7 ppb Ir and Pd, 0.05–1.4 ppb Ru, 0.01–0.2 ppb Rh, and 0.06–1.1 ppb Pt. All samples have high Cu/Pd ratios ranging from ~69,000 to 3,500,000, and low Cu/Zr ratios ranging from 0.1 to 0.8, suggesting sulfur-saturated fractionation. Model calculations indicate that the basalts are depleted in PGE due to the retention of 0.001% to 0.1% sulfide in the mantle and the removal of up to 0.0022% sulfide during magma ascent. The crystallization of olivine and spinel, and partial melting are insufficient to account for the observed PGE variation in these basalts. Thus, the distinct PGE patterns in basalts with different ages may reflect the heterogeneity of the mantle source beneath SE China. The source heterogeneity may be due to compositional heterogeneity, particularly variations in oxygen fugacity and PGE mineral phases, or due to variable fluid/melt metasomatic agents in the sub-continental lithospheric mantle. This heterogeneity is possibly related to the westward subduction of the Paleo-Pacific Plate.

1. Introduction

Cenozoic volcanic rocks are widespread in eastern China and cover an area of ~43,000 km^2 (Chen et al., 2014). They are part of the circum-Pacific volcanic belt located west of the calc-alkaline volcanic arcs in Japan, Izu–Bonin–Mariana, and the Philippines, and are closely associated with major regional faults (Zhou and Armstrong, 1982). These volcanic rocks are almost exclusively basalts of various types, with minor amounts of more fractionated lavas. Their lithophile trace element and isotopic compositions indicate that the Cenozoic basalts in SE China were derived from a mixture of asthenospheric mantle and enriched mantle 2 (EM2). In contrast, their equivalents in NE China were derived from a mixture of asthenospheric mantle and enriched mantle 1 (EM1), and are generally ocean island basalt (OIB)-like (Ho et al., 2003; Zou et al., 2000). Cenozoic basalts with varying ages in SE China are distributed along major NE-trending faults. Understanding whether these basalts are derived from the same mantle source or different sources is important to understand the evolution of the mantle beneath SE China.

Chalcophile elements, including platinum-group elements (PGEs), Ni and Cu, are commonly used to investigate the origin and evolution of mafic–ultramafic rocks, particularly to study sulfur-saturation and mineral fractionation processes (Barnes et al., 1985; X.-W. Huang et al., 2013; Momme et al., 2003; Philipp et al., 2001; Qi and Zhou, 2008; Qi et al., 2008; Wang et al., 2007, 2011; Yang et al., 2011; Zeng et al., 2016; Zhou et al., 1998). Moreover, PGE compositions of basalts can provide information about the nature of mantle sources such as DMM, EM2 and subduction-enriched mantle, which complements information from lithophile element tracers (Dale et al., 2008). The PGE geochemistry of basalts and peridotite xenoliths from Hannuoba in North China indicates a depletion of Ir relative to other PGEs (Chu et al., 1999). Ir-depleted mantle xenoliths have also been found elsewhere in NE China, and this Ir depletion is thus interpreted as a feature of the upper mantle beneath eastern China (Chu et al., 1999; Orberger et al., 1998; Xu et al., 1998; Zheng et al., 2005). However, mantle xenoliths in Nushan in the central part of eastern China show PGE patterns with no significant Ir depletion (Liu et al., 2010). Basalts from Leiqiong (Hainan province) and Sanshui (Guangdong province), and andesites from Lianping (Guangdong province) in SE China also lack a strong Ir-depletion, which has been attributed to derivation from a more oxidized sub-continental lithospheric mantle (SCLM; Yang et al., 2011).

* Corresponding author.
E-mail address: mfzhou@hku.hk (M.-F. Zhou).

http://dx.doi.org/10.1016/j.lithos.2017.03.016
0024-4937/

Therefore, the PGE variations in Cenozoic basalts may reflect heterogeneous mantle sources beneath eastern China.

In this study, we present new major and trace element data, and PGE data, for Cenozoic basalts from Mingxi and Niutoushan in Fujian province, Xilong in Zhejiang province, and Penghu in the Taiwan Strait. These new data are used to investigate the factors controlling PGE composition, sulfur saturation, and the nature of their mantle sources. Combined with previously reported PGE data from the Sanshui and Leiqiong basalts, this enables us to discuss the heterogeneity of the mantle source beneath SE China.

2. Geological background and sampling strategy

At the East Asia continental margin, the westward subduction of the Pacific plate and the northward indentation of India extend over 5000 km from Siberia over Eastern China to Indo-China. These two major tectonic processes are thought to govern the development of Cenozoic extensional basins and associated volcanic rocks in East Asia (Fan and Hooper, 1991; Tapponnier et al., 1982; Zhou and Armstrong, 1982).

The Cenozoic continental extension around the Taiwan Strait has resulted in basaltic volcanism in the Fujian–Taiwan region (Chung et al., 1994; Fig. 1). This extension is almost certainly related to the opening of the South China Sea (Nanni et al., 2017 and references therein), which in turn most likely resulted from the India–Eurasia collision (Tapponnier et al., 1982). The tensional forces formed numerous NE-trending sedimentary basins around the South China Sea, and tension may have propagated northeastwards to the Fujian–Taiwan region (Chung et al., 1994; Fig. 1). From east to west, three NE–SW trending volcanic belts have been identified in Guangdong, Fujian, and Zhejiang provinces, where these belts are associated with major faults (Chung et al., 1994; Qi et al., 1994; Zou et al., 2000; Fig. 1). The basalts in these belts yield ages ranging from the early Tertiary to the Pliocene. The basalts from Penghu near Taiwan are considered to be the product of passive extension around the Taiwan Strait, also in response to extension in the South China Sea (Tu et al., 1992; Xu et al., 2012).

In this study we collected samples of basalts from Mingxi (4.9–1.4 Ma) and Xilong (Pliocene to Pleistocene) in the western belt, from Niutoushan (17.9–16.7 Ma) in the central belt, and from Penghu (16.2–9.2 Ma) in the eastern belt (Chen and Zhang, 1992; Ho et al., 2003; Juang and Chen, 1992; Liu et al., 1992). These basalts usually contain mantle xenoliths, which are spinel and/or garnet peridotites. The phenocrysts in these basalts are dominantly olivine and clinopyroxene, with minor plagioclase, whereas the matrix is composed mainly of fine-grained plagioclase, olivine, clinopyroxene, and Fe–Ti oxides. Detailed petrographic descriptions of the basalts from Mingxi, Xilong, and Niutoushan can be found in Qi et al. (1994), and a detailed petrographic description of the Penghu basalts is provided by Juang and Chen (1999).

3. Analytical methods

Whole-rock major elements, trace elements, and PGEs were determined at the State Key Laboratory of Ore Deposit Geochemistry, Institute of Geochemistry, Chinese Academy of Sciences (IGCAS), Guiyang, China. The major element compositions of the Penghu basalts were analyzed at the Department of Earth Sciences, University of Hong Kong (HKU). Whole-rock major oxides were analyzed on fused glass beads using Panalytical Axios PW4400 (IGCAS) and Philips PW2400 (HKU) X-ray fluorescence spectrometers. Analytical uncertainties are better than 5%. Trace elements were analyzed using a PE Elan DRC-e ICP–MS after HF + HNO_3 digestion in a sealed Teflon beaker following the procedures of Qi et al. (2000). Precisions for most trace elements are typically better than 5%.

Whole-rock PGEs were determined by isotope dilution (ID)–ICP–MS (PE Elan DRC-e) using a modified digestion method (Qi et al., 2011). Five grams of rock powder (>200 mesh) and appropriate amounts of isotope spikes ^{101}Ru, ^{193}Ir, ^{105}Pd, and ^{194}Pt were weighed and then decomposed in a 120 ml sealed PTFE beaker by a mixture of HF and HNO_3 at 190 °C for 24 h. The solutions were evaporated to dryness and concentrated HCl was added. After drying, the solutions were conditioned to 2 N HCl and transferred to 50 ml centrifuge tubes. After centrifuging, the supernatant was transferred to the original beaker and used to preconcentrate PGEs by Te-coprecipitation. The main interfering elements (e.g., Cu, Ni, Zr, and Hf) were removed by a mixed ion exchange column that contained a Dowex 50W X8 cation exchange resin and a P507 levextrel resin.

Iridium, Ru, Pt, and Pd were measured by the isotope dilution method and the content of Rh was calculated using ^{194}Pt as an internal standard (Qi et al., 2004). The total procedural blanks were lower than 0.009 ng for Ru, Rh, and Ir, and lower than 0.030 ng for Pt and Pd. The analytical results obtained for the standard reference materials WGB-1 (gabbro) and TDB-1 (diabase) are in good agreement with certified

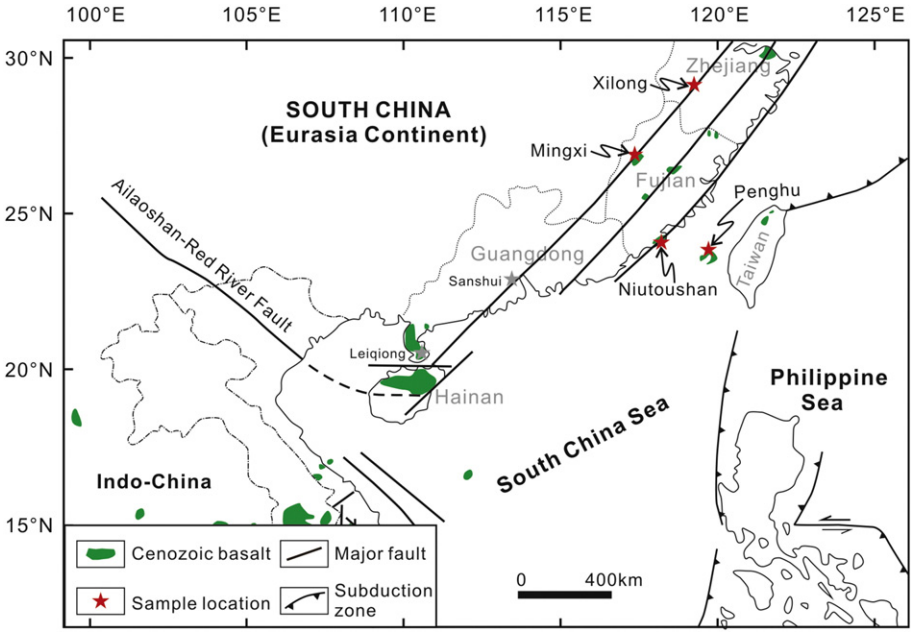

Fig. 1. Sketch map showing the tectonic framework of South China and adjacent areas (X.-L. Huang et al., 2013; Xu et al., 2002). The red stars mark the sample localities of this study. (For interpretation of the references to color in this figure legend, the reader is referred to the web version of this article.)

Table 1
Analytical results of PGE for standard materials TDB-1 and WGB-1.

Elements	TDB-1 (diabase)			WGB-1 (gabbro)		
	Average (1σ, n = 2)	Meisel	Certified	Average (1σ, n = 2)	Meisel	Certified
Ir	0.087 ± 0.033	0.075	0.15	0.25 ± 0.08	0.211	0.33
Ru	0.31 ± 0.01	0.198	0.3	0.24 ± 0.05	0.144	0.3
Rh	0.45 ± 0.06	0.471	0.7	0.36 ± 0.01	0.234	0.32
Pt	5.05 ± 0.22	5.01	5.8	6.05 ± 0.48	6.39	6.1
Pd	21.0 ± 1.2	24.3	22.4	13.4 ± 0.5	13.9	13.9

Meisel = Meisel and Moser (2004); Certified = Govindaraju (1994).

values (Table 1). Duplicate analyses of sample XL12-21 yielded a good reproducibility (Table 2).

4. Analytical results

4.1. Whole-rock major and trace elements

The major element data and most trace element data are available in the online Appendix, and Ni, Cu, and Zr contents are listed in Table 2. The basalts from the western, central, and eastern belts show different major element compositions. Basalts from the western belt have the lowest SiO_2 and Al_2O_3 contents, and the highest TiO_2, K_2O, and P_2O_5 contents, whereas those from the central belt have the highest SiO_2 and Al_2O_3 contents and the lowest contents of other oxides (Fig. 2). The basalts from the eastern belt have oxide contents that are intermediate between those from the other two belts. Due to the limited variance of MgO in the basalts from the western belt, there are no obvious correlations between MgO and other element oxides for basalts in this belt. On Harker diagrams, SiO_2, TiO_2, and Al_2O_3 show moderately negative correlations with MgO for the basalts from the central belt (Fig. 2a–c). The constant CaO/Al_2O_3 ratio for the basalts from the central belt with variable MgO indicates the fractional crystallization of olivine (Fig. 2f). The positive correlation between CaO/Al_2O_3 and MgO for the basalts from the western and eastern belts indicates the fractionation of clinopyroxene during differentiation (Fig. 2f). According to their major element composition, basalts from Niutoushan and Penghu are classified as tholeiites, whereas those from Mingxi and Xilong belong to the alkaline series.

All of the analyzed basalts show similar chondrite-normalized REE patterns with a relative LREE enrichment (Fig. 3a, c, e). The basalts from the western belt have the highest ∑REE contents (324–410 ppm), whereas those from the central belt have the lowest ∑REE contents (58.1–79.4 ppm) and those from the eastern belt have intermediate

Table 2
Nickel, Cu, Zr (ppm) and PGE (ppb) concentrations of basalts from SE China.

Sample no.	Ni	Cu	Zr	Ir	Ru	Rh	Pt	Pd	Cu/Ni	Cu/Zr	Cu/Pd
Niutoushan tholeiitic basalt											
NTS12-01	143	68	100	0.033	0.110	0.018	0.083	0.131	0.5	0.7	518,956
NTS12-02	128	67	103	0.023	0.089	0.016	0.065	0.132	0.5	0.7	512,192
NTS12-03	526	55	78	0.603	1.416	0.175	1.087	0.265	0.1	0.7	206,029
NTS12-05	358	57	86	0.217	0.529	0.101	0.566	0.298	0.2	0.7	189,826
NTS12-06	124	69	104	0.015	0.069	0.009	0.059	0.019	0.6	0.7	3,577,945
NTS12-07	297	61	92	0.141	0.386	0.050	0.254	0.152	0.2	0.7	399,575
NTS12-08	110	66	102	0.015	0.069	0.010	0.065	0.019	0.6	0.6	3,415,079
NTS12-09	120	66	105	0.015	0.089	0.021	0.062	0.087	0.5	0.6	756,440
NTS12-10	138	66	96	0.028	0.098	0.028	0.109	0.138	0.5	0.7	475,034
NTS12-11	147	68	105	0.023	0.120	0.015	0.096	0.049	0.5	0.7	1,392,381
NTS12-12	171	62	98	0.038	0.137	0.022	0.119	0.147	0.4	0.6	419,635
NTS12-13	214	63	88	0.084	0.197	0.026	0.200	0.174	0.3	0.7	359,837
NTS12-14	192	69	99	0.052	0.120	0.021	0.139	0.074	0.4	0.7	923,990
NTS12-15	279	62	93	0.139	0.381	0.074	0.384	0.195	0.2	0.7	318,544
NTS12-16	361	60	90	0.269	0.564	0.096	0.566	0.277	0.2	0.7	216,379
NTS12-19	227	63	94	0.121	0.184	0.043	0.302	0.211	0.3	0.7	297,782
NTS12-28	155	74	104	0.044	0.085	0.021	0.093	0.050	0.5	0.7	1,480,218
Xilong alkaline basalt											
XL12-21	380	50	308	0.289	0.649	0.187	0.957	0.722	0.1	0.2	69,054
XL12-21 replicate				0.296	0.670	0.180	1.158	0.852			
XL12-22	335	48	295	0.276	0.547	0.196	0.873	0.669	0.1	0.2	71,074
XL12-23	361	50	317	0.253	0.472	0.215	0.868	0.705	0.1	0.2	70,631
XL12-24	346	51	302	0.248	0.463	0.229	0.816	0.605	0.1	0.2	84,614
XL12-27	313	48	304	0.234	0.521	0.119	0.838	0.585	0.2	0.2	82,399
Mingxi alkaline basalt											
MX12-01	269	43	370	0.330	0.477	0.140	0.715	0.494	0.2	0.1	87,662
MX12-02	269	46	368	0.325	0.433	0.168	0.796	0.591	0.2	0.1	77,136
MX12-03	243	44	364	0.268	0.321	0.125	0.583	0.401	0.2	0.1	110,534
MX12-12	242	41	363	0.281	0.274	0.119	0.594	0.418	0.2	0.1	97,157
MX12-14	268	45	372	0.329	0.429	0.185	0.738	0.479	0.2	0.1	93,374
MX12-18	283	43	374	0.316	0.397	0.162	0.638	0.412	0.2	0.1	104,263
MX12-21	300	49	289	0.310	0.328	0.179	0.732	0.556	0.2	0.2	88,201
MX12-22	283	51	291	0.292	0.342	0.164	0.711	0.569	0.2	0.2	88,960
MX12-23	288	48	293	0.273	0.335	0.188	0.709	0.547	0.2	0.2	87,006
Penghu tholeiitic basalt											
20130601-1	128	77	157	0.019	0.076	0.009	0.079	0.076	0.6	0.5	1,014,956
20130601-2	147	58	206	0.020	0.052	0.009	0.173	0.140	0.4	0.3	418,233
20130602-1	142	43	241	0.020	0.059	0.014	0.284	0.197	0.3	0.2	218,043
20130602-2	147	58	240	0.023	0.072	0.017	0.236	0.221	0.4	0.2	262,016
20130602-3	143	63	80	0.016	0.052	0.006	0.065	0.066	0.4	0.8	958,877
20130603-2	166	56	199	0.049	0.108	0.034	0.366	0.340	0.3	0.3	164,360
20130603-5-1	184	70	182	0.056	0.148	0.034	0.421	0.540	0.4	0.4	129,187
20130603-5-2	200	65	185	0.069	0.260	0.059	0.359	0.475	0.3	0.4	137,067
20130603-6	167	55	199	0.047	0.118	0.029	0.328	0.319	0.3	0.3	172,884

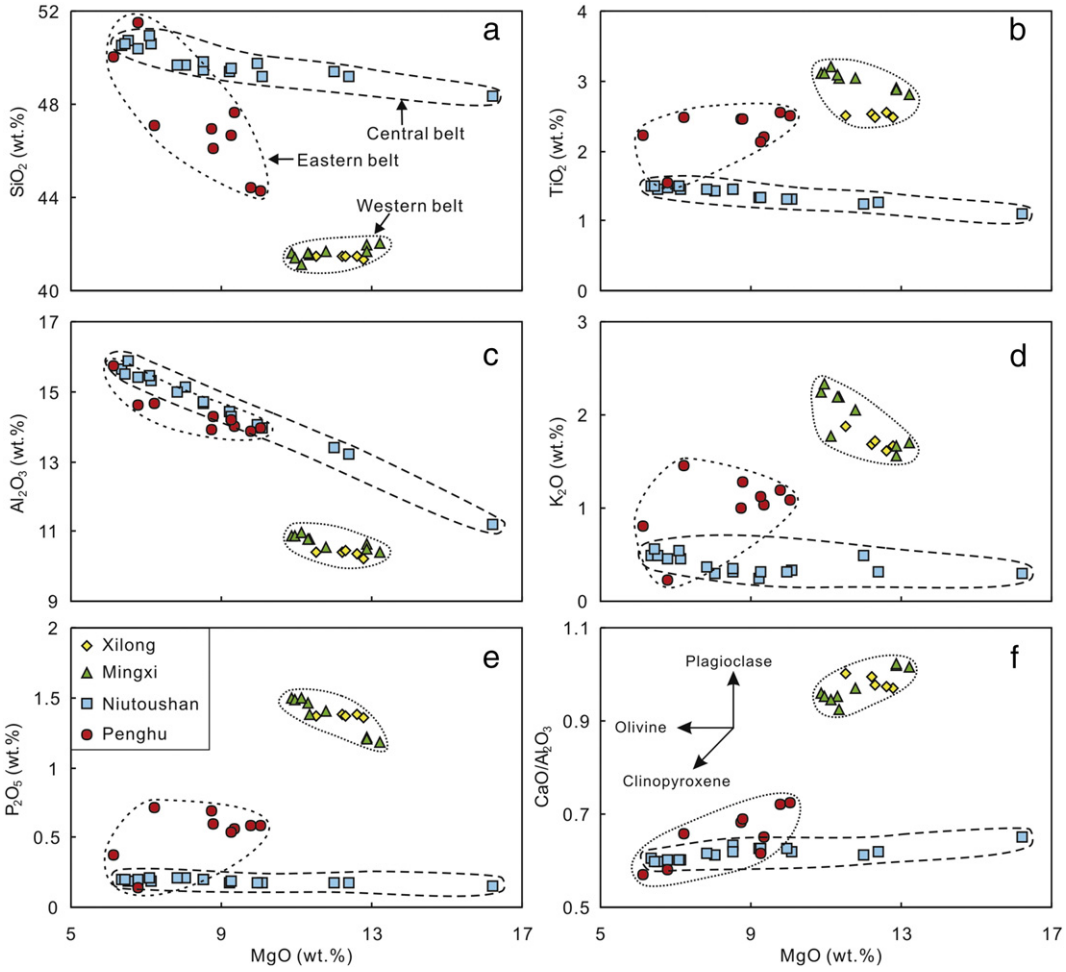

Fig. 2. Harker diagrams showing MgO versus SiO_2, TiO_2, Al_2O_3, K_2O, P_2O_5, and CaO/Al_2O_3 for basalts in SE China.

∑REE contents (51.6–214 ppm). The lack of negative Eu anomalies in all basalts indicates that plagioclase was not a major phase involved in fractional crystallization. Weakly positive Eu anomalies in basalts from the western belt are consistent with the presence of minor plagioclase megacrysts. The absence of a negative Ce anomaly indicates that these basalts are generally unaffected by low-temperature alteration. Most of the basalts have REE patterns similar to OIB, although a minority of the basalts from the eastern belt have REE patterns similar to E-MORB, with a slight LREE enrichment (Fig. 3a, c, e). The trace elements in most basalts exhibit OIB-like patterns, with enrichment of large ion lithophile elements (LILEs) and high field strength elements (HFSEs), a strong depletion of K and slightly positive Ta, P, and Ti anomalies (Fig. 3b, d, f). Some basalts from the eastern belt have trace element patterns similar to E-MORB. All basalts have trace element patterns that are different from island arc volcanic rocks and continental crustal rocks, which are commonly characterized by negative Nb and Ta anomalies, and positive Pb anomalies.

4.2. Whole-rock chalcophile elements

The basalts from the western belt contain 240–380 ppm Ni and 40–51 ppm Cu with relatively constant Cu/Ni ratios of 0.1–0.2 (Table 2). Those from the central belt have more variable Ni and Cu contents ranging from 110 to 526 ppm and from 55 to 74 ppm, respectively, with Cu/Ni ratios of 0.1–0.6. The basalts from the eastern belt have Ni and Cu contents similar to those from the central belt and have Cu/Ni ratios of 0.3–0.6 (Table 2). All basalts have Ir, Ru, Rh, Pt, and Pd contents that are mostly below 1 ppb (Table 2). The PGE contents in basalts from the western belt are slightly higher than those of basalts from the other two belts.

The basalts from the central and eastern belts show positive correlations between Ir and other PGEs (Fig. 4a–d). Conversely, basalts from the western belt show no obvious correlation between Ir and other PGEs, due to the limited variation in PGE contents. Except for a few outliers, all basalts have Pd/Ir ratios between ~1.3 and 10, exceeding the primitive mantle ratio of ~1.2 (Barnes and Maier, 1999; Fig. 4d). Platinum also shows a positive correlation with Pd in basalts from all belts (Fig. 4e). The basalts from the western and eastern belts have Pt/Pd ratios of 0.8 to 1.5, slightly lower than the primitive mantle ratio of ~1.8 (Fig. 4e), whereas the basalts from the central belt have more variable Pt/Pd ratios of 0.5 to 4.1 (Fig. 4e). The basalts from the central and eastern belts show positive correlations between PGEs and MgO, and between PGEs and Cr (Fig. 5). These trends are not obvious for the basalts from the western belt due to the small variation in their PGE contents. On the primitive-mantle-normalized siderophile and chalcophile element diagram (Ni, PGEs, and Cu), basalts from the three belts show W- or U-shaped patterns with depletion of PGEs relative to Ni and Cu (Fig. 6a).

5. Discussion

5.1. Roles of olivine and spinel fractionation

The constant CaO/Al_2O_3 ratio with variable MgO content for the basalts from the central belt could indicate the fractionation of olivine (Fig. 2f). Positive correlations of Ir and Ru with MgO and Cr for the basalts from the central belt indicate that Ir and Ru were likely compatible during the fractionation of olivine and spinel (Fig. 5a, b, f, g). Because Pd

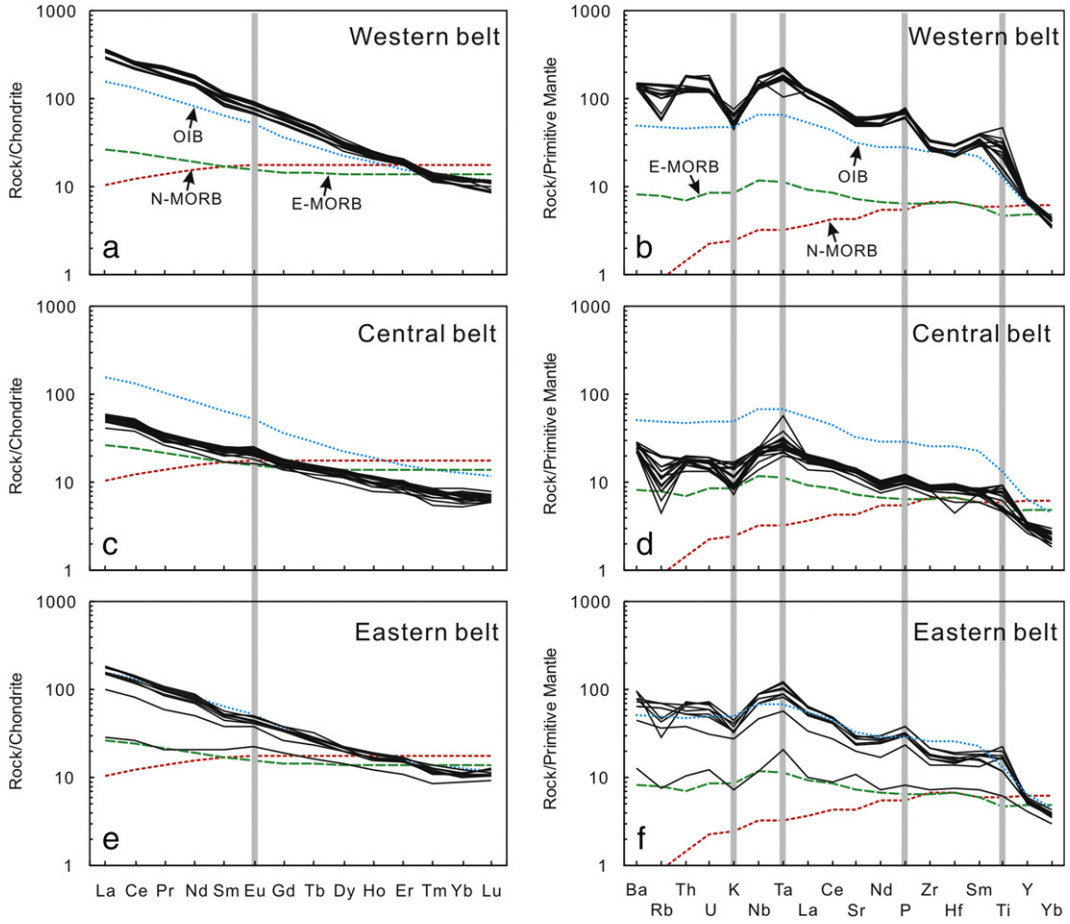

Fig. 3. Chondrite-normalized REE patterns (a, c, e) and primitive-mantle-normalized trace element patterns (b, d, f) for basalts in SE China. Normalization values and E-MORB, N-MORB, and OIB data are from Sun and McDonough (1989). The gray lines highlight the relative enrichment or depletion of some elements.

is incompatible and Ir is compatible in olivine or spinel (Barnes et al., 1985), Pd/Ir ratios will increase during S-undersaturated differentiation. The basalts from the central belt show weakly negative correlations between Pd/Ir and MgO and between Pd/Ir and Cr (Fig. 7a and b), indicating that fractional crystallization of olivine and spinel had a slight effect on Pd–Ir fractionation. The basalts from the western and eastern belts show relatively constant Pd/Ir ratios when plotted versus indicators of magma differentiation, suggesting that fractional crystallization of these minerals has a negligible influence on the fractionation of IPGE from PPGE. This inference is also supported by a plot of Cu/Ni versus Pd/Ir (Fig. 7c), in which the basalts from the central belt show a weakly positive correlation between these ratios, whereas those from the western and eastern belts show no obvious correlations. Because both Ni and Ir are more compatible than Cu and Pd in olivine and spinel (Puchtel and Humayun, 2001; Righter et al., 2004), fractional crystallization of these minerals would increase Pd/Ir and Cu/Ni ratios in concert. Moreover, the lack of an obvious negative correlation between Pd and MgO or Cr for basalts from all three belts (Fig. 5e, j) indicates that the fractional crystallization of olivine and spinel was not the main factor controlling their PGE compositions.

5.2. Role of partial melting

PGE variations can also result from partial melting (Keays, 1995). Due to the different compatibilities of the various PGEs, a variation in the degree of melting would produce different PGE ratios. For example, if the La/Sm ratio is taken as an indicator of the degree of partial melting, the Pd/Ir ratio would increase with increasing melt fraction, as shown in a suite of basalts from the Reunion hotspot trace (ODP Leg 115; Greenough and Fryer, 1990; Greenough and Owen, 1992). In the basalts from the central belt, the Pd/Ir ratios span nearly an order of magnitude for a given La/Sm ratio of ~4 (Fig. 8a), suggesting that the Pd–Ir systematics are decoupled from the degree of melting. However, positive correlations between Pd/Ir and La/Sm ratios for the basalts from the western and eastern belts (Fig. 8a) indicate that fractionation of PPGE from IPGE was partly affected by the degree of partial melting. The absence of correlations between La/Sm and Ru/Ir or Pt/Pd for all basalts (Fig. 8b and c) implies that PGE fractionation was not controlled by partial melting. Therefore, partial melting had a slight effect on the PGE composition of the basalts from the western and eastern belts, but not on those from the central belt.

It is commonly suggested that most alkali basalts are generated by a relatively low degree of partial melting of enriched mantle sources at high pressure, within plumes ascending from a deep-seated mantle reservoir, whereas tholeiites form by higher degrees of melting at lower pressures (Jaques and Green, 1980; Yoder and Tilley, 1962). High-degree melts such as high-Mg tholeiites and komatiites are expected to have lower Pd/Ir and higher Pt/Pd ratios than low-degree melts such as alkali basalts, particularly if the magmas are derived from a similar source. The lower degrees of partial melting inferred for alkaline basalts from the western belt compared with tholeiites from the central and eastern belts are consistent with the higher contents of incompatible elements (e.g., Nb, Th, La, and Nd) in the basalts from the western belt (Fig. 3). However, alkaline basalts from the western belt have much lower Pd/Ir ratios and higher Pt/Pd ratios than the tholeiites from the eastern belt (Fig. 8a and c). This indicates that the degree of partial melting alone cannot explain the PGE variations between basalts from different belts.

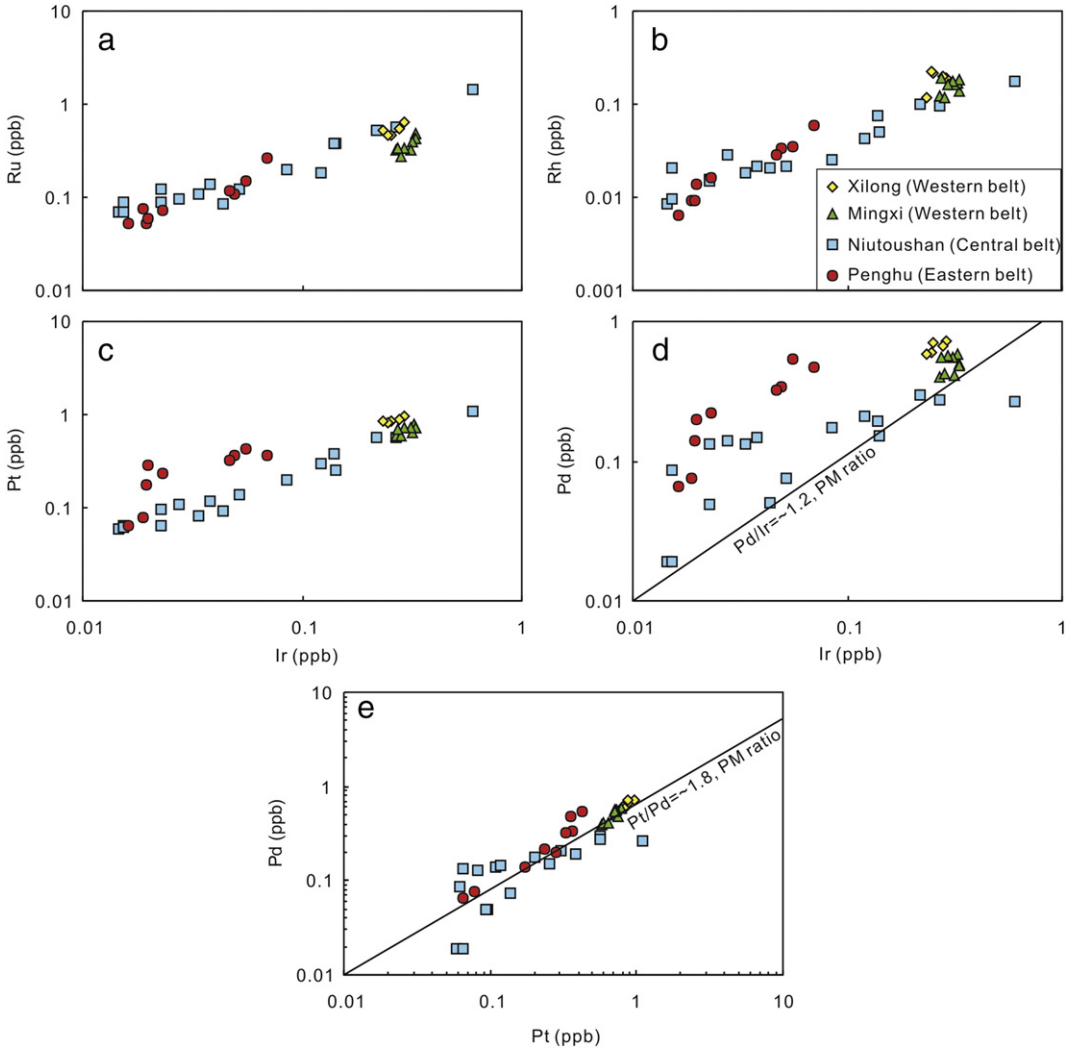

Fig. 4. Plots of Ir versus Ru, Rh, Pt, and Pd, and Pt versus Pd for basalts in SE China. The lines show PGE ratios of primitive mantle (Barnes and Maier, 1999).

In summary, both partial melting and fractional crystallization of olivine and spinel cannot account for the PGE variations of basalts from the three belts. Alternative geological processes should thus be considered to explain this variation.

5.3. Role of sulfide segregation

Palladium and iridium have comparable silicate melt–sulfide melt partitioning coefficients (Fleet et al., 1991; Peach et al., 1994), and thus show similar compatible behavior during S-saturated differentiation. Positive correlations between Ir and other PGEs (Fig. 4) and between PPGE, MgO, and Cr (Fig. 5d, e, I, j) in these basalts indicate S-saturated differentiation. The PGE depletion relative to Ni and Cu for basalts from the three belts (Fig. 6) also implies sulfide removal/saturation in the mantle source and/or during magma differentiation (Barnes et al., 1985; Fleet et al., 1991).

The Cu/Zr ratios can also be used to examine sulfide segregation. Typically, mafic magmas that are not depleted in chalcophile metals have Cu/Zr ratios around 1, whereas magmas that experienced sulfide segregation have Cu/Zr ratios lower than unity due to the high compatibility of Cu in sulfide (Lightfoot and Keays, 2005). The Cu/Zr ratios of the basalts from the three belts range from 0.1 to 0.8, reflecting the removal of sulfide during magmatic differentiation. The basalts from the western and eastern belts show a positive correlation between Cu and Cu/Zr ratios (Fig. 9a) and a negative correlation between Zr and Cu/Zr ratios (Fig. 9b), which is typical for S-saturated fractionation. The basalts from the central belt have relatively constant Cu/Zr ratios of ~0.7 and lack correlations with Cu or Zr (Fig. 9a and b), and a trend of olivine fractionation is consistent with their major element variation (Fig. 2f).

Because Cu is much less chalcophile than Pd (Barnes and Maier, 1999), the Cu/Pd ratio should increase if sulfide is fractionated from a magma, and thus constitutes a useful indicator of sulfide fractionation. On the other hand, if a suite of magmas fractionates silicate, spinel, and perhaps platinum-group minerals (PGMs) instead of sulfur, the Cu/Pd ratio should be constant. The basalts from the western, central, and eastern belts have Cu/Pd ratios ranging from 69,000 to 110,000, ~190,000 to 3,600,000, and 129,000 to 1,000,000, respectively (Fig. 9c and d), all of which are highly variable and considerably higher than the mantle value of ~7000 (Barnes and Maier, 1999), indicating S-saturated fractionation.

5.3.1. Sulfur-saturated melting of a mantle source

Whether or not magmatic sulfides are retained during partial melting of the mantle has a critical influence on the PGE contents of the resulting melts (Barnes et al., 2015). The presence of even minor residual sulfide is enough to produce a strong PGE depletion in mantle melts that are sulfide-saturated in the source region (Hamlyn and Keays, 1986; Mungall and Brenan, 2014). The PGE budget of a primary

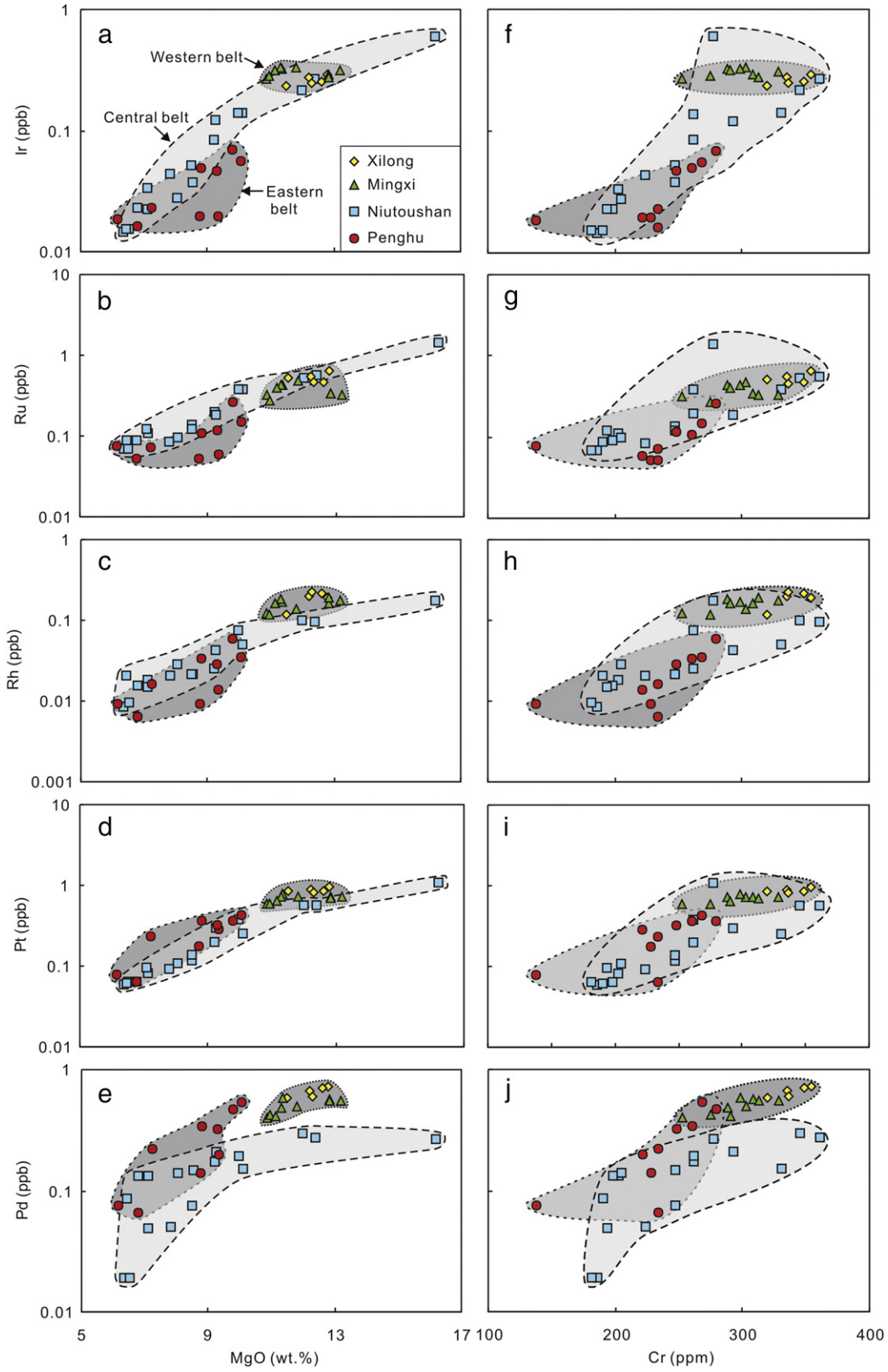

Fig. 5. Plots of Ir, Ru, Rh, Pt, and Pd versus MgO and Cr for basalts in SE China.

magma depends on the degree of partial melting and on the sulfur concentration in the mantle source. The PGEs would be retained in the mantle source during a small degree of partial melting under S-undersaturated conditions, in which sulfides remain in the mantle because of their high sulfide/silicate melt partition coefficients (Fleet et al., 1991; Keays, 1995). In a columnar melting regime, at least ~25% of partial

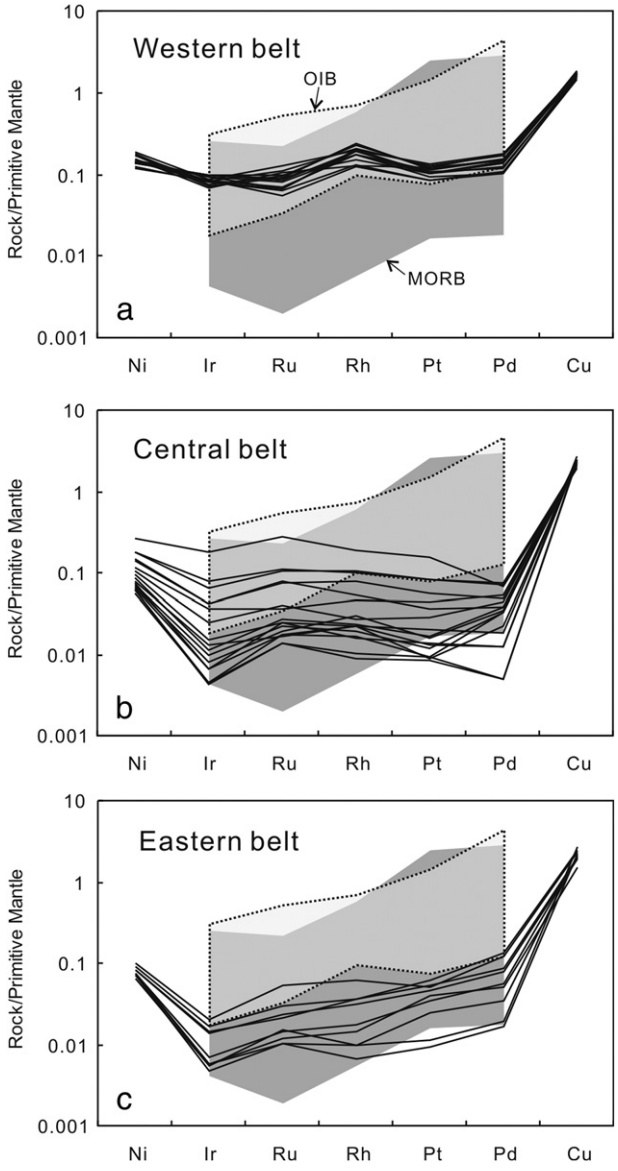

Fig. 6. Primitive-mantle-normalized PGE patterns of basalts in SE China. Normalization values are from Barnes and Maier (1999). PGE contents of MORB and OIB are from Barnes et al. (2015).

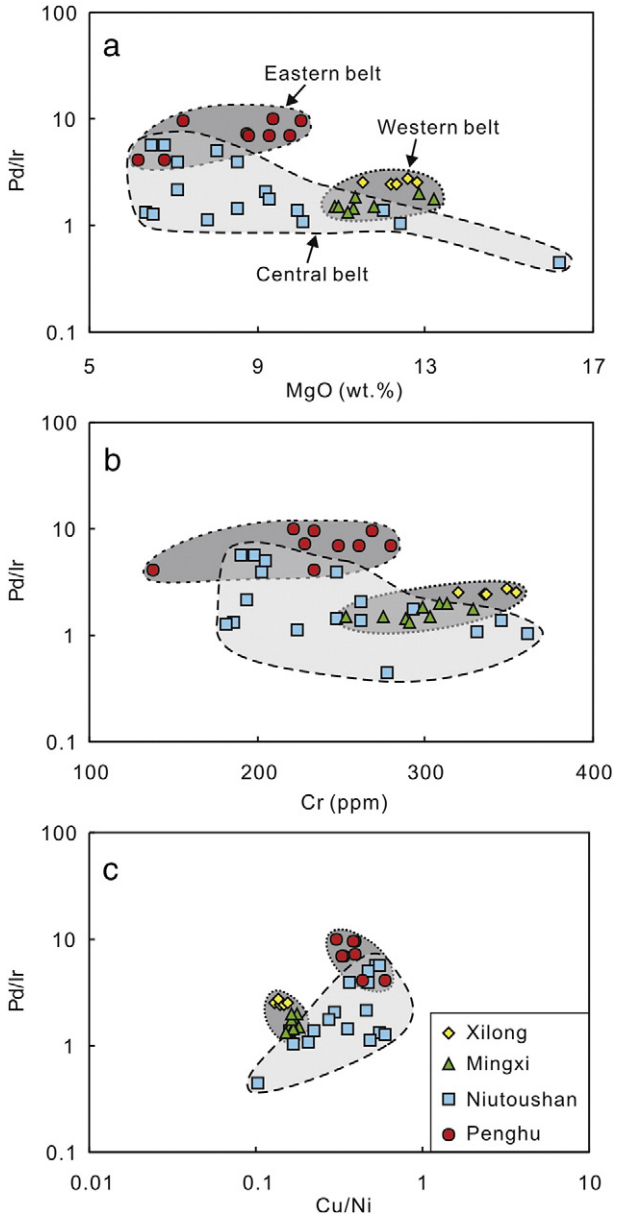

Fig. 7. Plots of Pd/Ir versus MgO, Cr, and Cu/Ni for basalts in SE China.

melting is required to produce S-undersaturated and PGE-undepleted primary magmas through complete exhaustion of sulfide in the mantle (Keays, 1995; Rehkämper et al., 1999).

Both the composition of the mantle source and the degree of partial melting that produced the parental magmas can be estimated using REE abundances and their ratios in basalts. Heavy rare earth elements (HREEs) are compatible in garnet, whereas the middle rare earth elements (MREEs) are incompatible or weakly compatible (Irving and Frey, 1978). In contrast, all REEs are strongly incompatible in spinel (Kelemen et al., 1990). Thus, basaltic magmas derived from a mantle source in the stability field of garnet will have Sm/Yb ratios higher than those generated from a mantle source where spinel is stable. In addition to mantle source discrimination, Sm/Yb and La/Sm ratios are commonly used to model the degree of partial melting of basaltic magma (Aldanmaz et al., 2000; Green, 2006). Our calculations reveal that the basalts from the western belt were derived from ~4% partial melting of a garnet lherzolite source (Fig. 10). The basalts from the central and eastern belts have a mixed source consisting of spinel and garnet lherzolites and formed from 4%–7% and 2%–3% partial melting, respectively (Fig. 10). The low degrees of partial melting for the basalts from the three belts indicate that some sulfides would have remained in the mantle source after melting. The relatively constant Cu/Pd ratios and the absence of correlations between Cu/Pd and MgO or Cr in the basalts from the western belt (Fig. 9c and d) suggest significant amounts of residual sulfides in the mantle source. Sulfur saturation in the source is also confirmed by the Re–Os isotopic compositions of sulfides in spinel peridotite xenoliths hosted by the Penghu basalts in the eastern belt (Wang et al., 2009).

5.3.2. Sulfide saturation during magma ascent

The very low PGE concentrations of the basalts in SE China cannot be explained by residual sulfide in the mantle source alone. The flat PGE patterns relative to Cu and Ni (Fig. 6) may indicate that the low PGE concentrations of the lavas can also be attributed to subsequent sulfide segregation during differentiation (Barnes et al., 1985). The 19-fold and 7-fold variations in Cu/Pd ratios for the basalts from the central and eastern belts, respectively, and the negative correlations of the Cu/Pd ratios with MgO and Cr (Fig. 9c and d) also indicate that these melts experienced sulfide segregation during magma ascent.

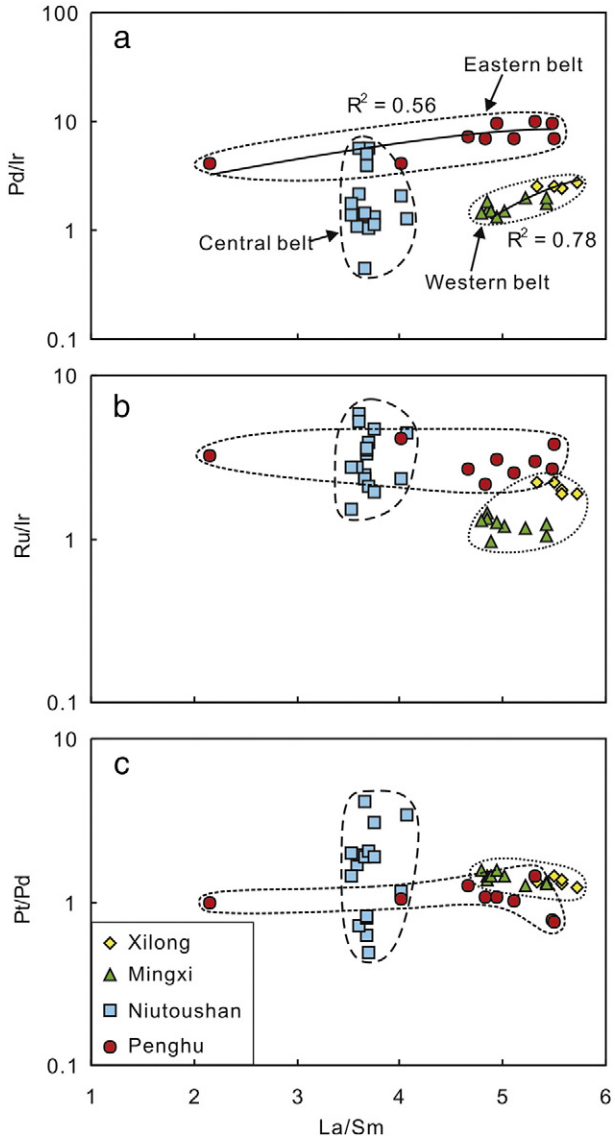

Fig. 8. Plots of La/Sm versus Pd/Ir, Ru/Ir, and Pt/Pd for basalts in SE China. The La/Sm ratio is used as an indicator of the degree of partial melting. Pd/Ir correlates with La/Sm for basalts from the eastern and western belts, with correlation coefficients (R^2) of 0.56 and 0.78, respectively. The Ru/Ir and Pt/Pd ratios of the basalts are not correlated with their La/Sm ratio, irrespective of the belt.

To quantitatively estimate the amount of immiscible sulfide removed, we used the plot of Cu/Pd versus Pd to model the sulfur saturation process (Fig. 11). For this model, we used the initial PGE composition of depleted MORB mantle (DMM) and selected different amounts of residual sulfides. Modeling results show that basalts from the western belt have 0.002%–0.01% sulfides retained in the source and did not experience sulfide separation during magma ascent. This is consistent with the relatively constant Cu/Pd ratios over a range of Mg and Cr contents in the basalts from the western belt (Fig. 9c and d). The basalts from the central and eastern belts indicate not only residual sulfide in the source (0.002%), but also up to 0.002% sulfide segregation during magma ascent. The modeling results are consistent with the covariations of the Cu/Zr ratio with Cu and Zr (Fig. 9a and b) and the covariation of the Cu/Pd ratio with MgO and Cr (Fig. 9c and d).

5.4. Nature of the mantle source

Siderophile and chalcophile element patterns of the studied basalts from the western, central, and eastern belts in SE China (Table 2 and Fig. 6) suggest that these basalts have different mantle sources and experienced different magmatic processes. From what has been discussed above, we can conclude that the PGE compositions of these basalts were inherited from their mantle sources.

For example, the basalts in drill core from the Philippine Sea Plate with EM2-type lithophile element chemistry show an extreme PGE fractionation with high Pt/Ir ratios, low Pd/Ir ratios, and anomalously high Ru/Ir ratios of >10 (Dale et al., 2008). The basalts in this study have OIB-like trace element patterns, but show no strong fractionation between Ru and Ir, unlike the EM2-type OIB. A similar decoupling of PGEs and lithophile elements is observed for the metasomatized continental peridotites of Somerset Island, Canada (Irvine et al., 2003) and in the Kimberley Craton, Australia (Luguet et al., 2009). All the studied basalts have PGE patterns similar to MORB (Fig. 6), indicative of a depleted mantle source. Moreover, the lithophile element geochemistry and Sr–Nd–Pb isotopic compositions of the basalts in SE China suggest mixing of a depleted asthenospheric mantle source with an EM2 component (Chung et al., 1994; Wang et al., 2012; Zou et al., 2000). The metasomatized SCLM has been proposed as a candidate for EM2 components (Han et al., 2009; Wang et al., 2009; Xu et al., 2003).

In mantle-derived rocks, some PGE ratios (e.g., Pt/Pd and Pd/Ir) are indicators of mantle metasomatism (Maier and Barnes, 2004). Basalts that form in fluid-rich melting regimes within a metasomatized lithospheric mantle may have Pt/Pd ratios of ~1–1.8 and Pd/Ir ratios of ~2–40, close to the chondritic ratios, whereas those derived from a mantle source without strong fluid/melt metasomatism commonly have sub-chondritic Pt/Pd and super-chondritic Pd/Ir ratios (Maier and Barnes, 2004). The basalts from the western belt have Pt/Pd and Pd/Ir ratios of 1.2–1.5 and 1.3–2.8, respectively, comparable to basalts from a metasomatized mantle source. The basalts from the central and eastern belts have Pt/Pd ratios of ~0.5–4.1 (average 1.5) and Pd/Ir ratios of ~0.4–10 (average 4.1), similar to those from a metasomatized mantle source (Maier and Barnes, 2004). However, the super-chondritic Pt/Pd ratios of some basalts from the central and eastern belts are different from those of basalts elsewhere (Maier and Barnes, 2004). The latter cannot be explained by fluid metasomatism and may be due to compositional heterogeneity in the mantle source. The Sanshui basalts in SE China have Pd/Ir ratios of 13–185 (Yang et al., 2011), which are atypical for mantle metasomatism, whereas the Leiqiong basalts have lower Pd/Ir ratios of 6–58 (Yang et al., 2011), which could be indicative of mantle metasomatism. Therefore, the PGE compositions of basalts suggest that the formation of the basalts in SE China may have involved a mantle source that experienced variable metasomatism by fluids/melts. Such fluid/melt metasomatism in the lithospheric mantle below SE China is also indicated by mantle xenoliths (Tatsumoto et al., 1992; Xu et al., 2003; Yu et al., 2006), and is thought to be related to the subduction of the Paleo-Pacific Plate (Tatsumoto et al., 1992) and/or the opening and post-spreading phase of the South China Sea (Yang et al., 2011; Yu et al., 2006).

5.5. Implications for mantle heterogeneity beneath SE China

The mantle source underneath SE China may have been compositionally heterogeneous (X.-L. Huang et al., 2013; Zou et al., 2000), because the basalts from different locations have various isotopic compositions (Fig. 12). The Niutoushan, Xilong, Mingxi, and Penghu basalts show limited variations in Sr–Nd isotope compositions, whereas the Sanshui and Leiqiong basalts show relatively large isotope variations (Fig. 12). The Sanshui basalts have higher $^{87}Sr/^{86}Sr$ ratios than the basalts from other locations. A common interpretation of such elevated $^{87}Sr/^{86}Sr$ ratios is that it represents the influence of subducted and seawater-altered oceanic crust in the source region of the magma (Zhou and Carlson, 1982). In addition to different Sr–Nd isotope compositions, the basalts from different belts show three different trends in plots of MgO versus SiO_2, TiO_2, Al_2O_3, K_2O, and P_2O_5 (Fig. 2a–e), further demonstrating that they were derived from different sources.

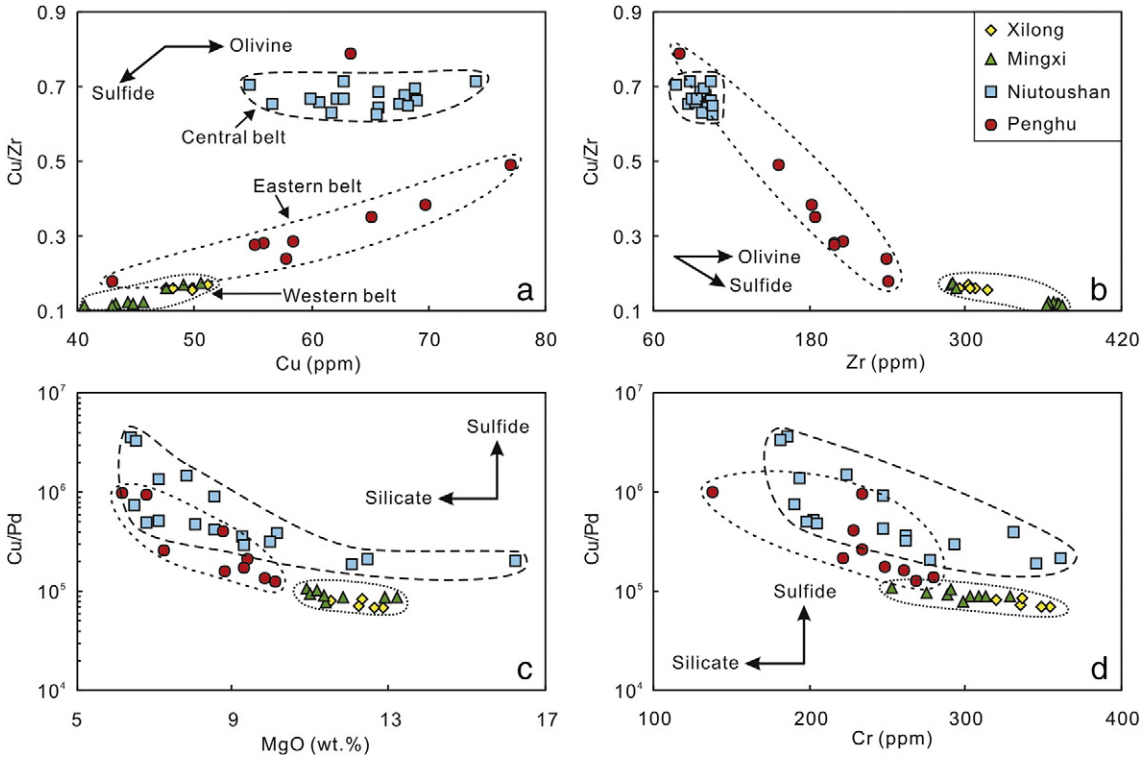

Fig. 9. Plots of Cu/Zr versus Cu and Zr, and Cu/Pd versus MgO and Cr for basalts in SE China.

Moreover, REE ratios indicate that the Xilong and Mingxi basalts were derived from a garnet lherzolite mantle, whereas those from Niutoushan, Penghu, Sanshui, and Leiqiong were derived from a garnet lherzolite mantle mixed with a spinel lherzolite mantle (Fig. 10). Thus, the combined geochemical and isotopic data indicate a considerable degree of heterogeneity in the Cenozoic mantle beneath SE China.

Cenozoic basalts from Niutoushan, Xilong, Mingxi, Penghu, Sanshui, and Leiqiong display PGE patterns that vary over time (Fig. 13). For example, the mid-Paleocene to mid-Eocene Sanshui basalts have lower PGE (particularly IPGE) contents than Miocene and Pliocene to Pleistocene basalts. The Sanshui basalts have smooth, inclined Ni–PGE–Cu patterns, which are a function of decreasing PGE compatibility from Ir to Pd (Fig. 13a) and are typical MORB-like patterns that indicate derivation from a depleted mantle source. This is consistent with the conclusion

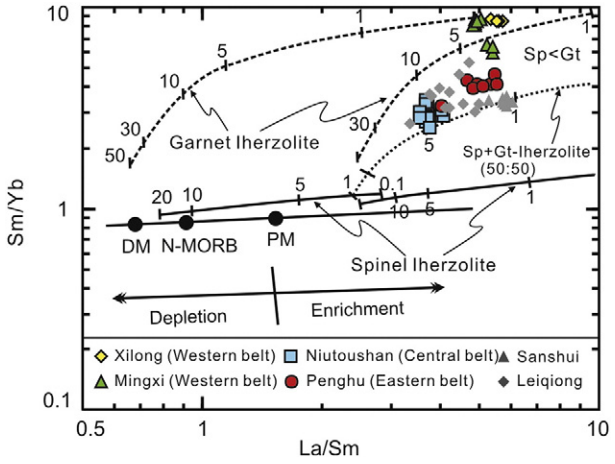

Fig. 10. Plot of Sm/Yb vs. La/Sm showing the partial melting degrees of basalts in SE China. The REE data for the Sanshui and Leiqiong basalts are from Yang et al. (2011). The melting curves for spinel lherzolite and garnet peridotite sources (lines) were obtained using the non-modal batch melting equations of Shaw (1970), employing the depleted MORB mantle (DMM) and primitive mantle (PM) compositions from Aldanmaz et al. (2000). The numbers on each melting curve correspond to the degree of partial melting (in percent) for a given mantle source. Mineral/matrix partition coefficients are from the compilation of McKenzie and O'Nions (1991, 1995). DMM compositions are from McKenzie and O'Nions (1991), whereas PM and E-MORB compositions are from Sun and McDonough (1989).

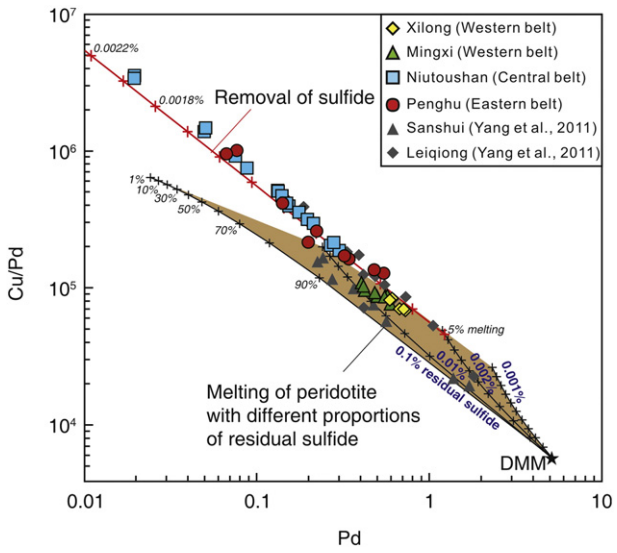

Fig. 11. Plot of Cu/Pd vs. Pd for basalts from Niutoushan, Xilong, Mingxi, and Penghu in SE China. The Sanshui and Leiqiong basalts from Yang et al. (2011) are also shown for comparison. The black curves represent simple batch-melting curves for peridotite with residual sulfide. Partition coefficients of olivine, clinopyroxene, orthopyroxene, and garnet for Pd are from Chazey and Neal (2005). Partition coefficients of olivine, clinopyroxene, orthopyroxene, and garnet for Cu are from Klock and Palme (1988), Hart and Dunn (1993), Klemme et al. (2006), and Yurimoto and Ohtani (1992), respectively. The partition coefficients of Pd and Cu in sulfide are from Mungall and Brenan (2014). The proportions of residual phase during the melting of eclogite are assumed to be modal (62% olivine, 14.9%–14.999% clinopyroxene, 15% orthopyroxene, 8% garnet, and 0.1%–0.001% sulfide). Data for DMM (depleted MORB mantle) are from Salters and Andreas (2004).

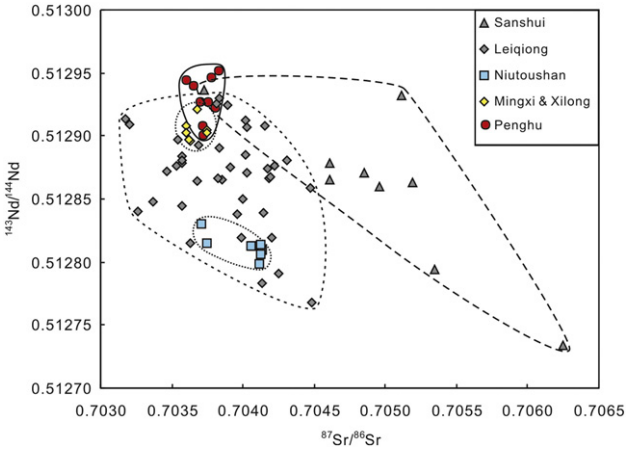

Fig. 12. Sr and Nd isotope compositions of basalts from Sanshui (Chung et al., 1997; Zhou et al., 2009), Leiqiong (Han et al., 2009; Tu et al., 1991), Penghu (Chung et al., 1994), Niutoushan, Mingxi, and Xilong (Zou et al., 2000) in SE China.

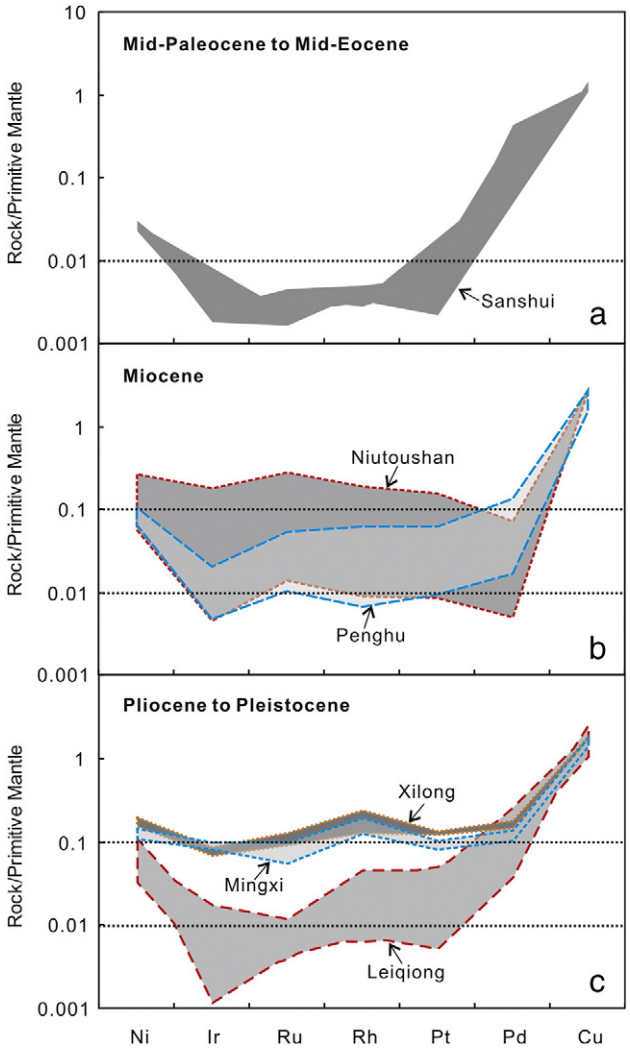

Fig. 13. Primitive-mantle-normalized Ni–PGE–Cu patterns of Cenozoic basalts in SE China. (a) Mid-Paleocene to mid-Eocene Sanshui basalts. (b) Miocene Niutoushan and Penghu basalts. (c) Pliocene to Pleistocene Xilong, Mingxi, and Leiqiong basalts. PGE data of the Sanshui and Leiqiong basalts are from Yang et al. (2011). Primitive mantle values are from Sun and McDonough (1989).

that the Sanshui basalts formed under relatively "dry" melting conditions without significant melt/fluid metasomatism. In addition, basalts of the same age show different PGE patterns at different localities. For example, the Miocene Niutoushan basalts are characterized by distinct Ir and Pd depletions, whereas the contemporaneous Penghu basalts have lower IPGE contents and a significant Ir depletion (Fig. 13b). The Pliocene to Pleistocene Mingxi and Xilong basalts show a relative enrichment in Rh, whereas the contemporaneous Leiqiong basalts have lower PGE contents and a slight Ir depletion (Fig. 13c). The variable PGE patterns in contemporaneous basalts demonstrate that the mantle beneath SE China has been heterogeneous during the entire Cenozoic. The distinct depletion of IPGE in these basalts may be related to the interplay between temperature, fO_2, alloy solubility, and partition coefficients during mantle melting (Barnes et al., 2015). Among these factors, fO_2 is the most important because it can control partition coefficients between melt, alloys, and olivine, as well as alloy solubilities via redox reactions between metals and dissolved oxide cations of various valence states (Barnes et al., 2015). The sulfide saturation level in mafic magmas increases with decreasing fO_2 (Carroll and Webster, 1994; Naldrett, 2004). Yang et al. (2011) suggested that differences in fO_2 conditions of the SCLM are the main cause for the PGE differences between the basalts in NE China and SE China; i.e., the presence or absence of Ir anomalies. Similarly, differences in oxygen fugacity may also explain the various degrees of Ir depletion in the basalts from SE China.

The spatially heterogeneous fO_2 conditions of the SCLM can explain the Ir depletion, but cannot account for the Pd depletion in the Niutoushan basalts. The Pd concentrations are largely controlled by Cu-rich sulfide, which has a relatively low melting temperature (Craig and Scott, 1974), facilitating its incorporation into the melt. Our current knowledge of PGE distribution in mantle phases precludes the depletion of Pd without influencing other PGEs or Re (Dale et al., 2008). However, refractory alloy phases that largely consist of Pd have not been documented. Furthermore, Pt readily forms alloys in the mantle that are more refractory than Pd-rich sulfide, meaning that low Pt/Pd ratios in melts would be more likely than the high Pt/Pd ratios observed here. Given these constraints, to generate basalts with the observed PGE features (e.g., the super-chondritic Pt/Pd ratios of the basalts in the central and eastern belts) the mantle source would have to contain phases that have not yet been documented. Therefore, the compositional heterogeneity of the SCLM, particularly in terms of oxygen fugacity and the presence of PGE mineral phases, and variable fluid/melt metasomatism may be responsible for the heterogeneity of the mantle source beneath SE China.

6. Conclusions

Basalts from the western, central, and eastern belts in SE China are PGE-depleted due to sulfur-saturation fractionation. Fractional crystallization and partial melting are not sufficient to explain the observed PGE variations in these basalts. These basalts have been derived from compositionally variable mantle sources with variable sulfide retention in the mantle and variable sulfide removal during magma ascent. The temporal PGE variations in these basalts may reflect the heterogeneity of the mantle source beneath SE China, which could be attributed to variable fluid/melt metasomatism in the SCLM, related to the subduction of the Paleo-Pacific Plate.

Supplementary data to this article can be found online at http://dx.doi.org/10.1016/j.lithos.2017.03.016.

Acknowledgments

This work was supported by the Research Grant Council of Hong Kong (HKU706413P) and an Open Grant from the State Key Laboratory of Ore Deposit Geochemistry, Institute of Geochemistry, Chinese Academy of Sciences, China (201403) to MFZ; and a grant from the Youth Innovation Promotion Association, Chinese Academy of Sciences, China

(Grant 2016067) to BXS. We thank Gang Zeng (Nanjing University) for assistance with the model calculations. We are thankful for thoughtful and constructive reviews by Editor Andrew Kerr, Zhuyin Chu, and an anonymous reviewer.

References

Aldanmaz, E., Pearce, J.A., Thirlwall, M.F., Mitchell, J.G., 2000. Petrogenetic evolution of late Cenozoic, post-collision volcanism in western Anatolia, Turkey. Journal of Volcanology and Geothermal Research 102, 67–95.

Barnes, S.J., Maier, W.D., 1999. The fractionation of Ni, Cu and the noble metals in silicate and sulphide liquids. In: Keays, R.R., Lesher, C.M., Lightfoot, P.C., Farrow, C.E.G. (Eds.), Dynamic Processes in Magmatic Ore Deposits and Their Application to Mineral Exploration. Geological Association of Canada, Short Course Notes, pp. 69–106.

Barnes, S.J., Mungall, J.E., Maier, W.D., 2015. Platinum group elements in mantle melts and mantle samples. Lithos 232, 395–417.

Barnes, S.J., Naldrett, A.J., Gorton, M.P., 1985. The origin of the fractionation of platinum-group elements in terrestrial magmas. Chemical Geology 53, 303–323.

Carroll, M.R., Webster, J.D., 1994. Solubilities of sulphur, noble gases, nitrogen, chlorine and fluorine in magma. Reviews in Mineralogy and Geochemistry 30, 231–279.

Chazey III, W.J., Neal, C.R., 2005. Platinum-group element constraints on source composition and magma evolution of the Kerguelen Plateau using basalts from ODP Leg 183. Geochimica et Cosmochimica Acta 69, 4685–4701.

Chen, X., Chen, L., Chen, Y., Zeng, G., Liu, J., 2014. Distribution summary of Cenozoic basalts in central and eastern China. Geological Journal of China Universities 20, 507–519 (in Chinese with English abstract).

Chen, D., Zhang, J., 1992. Nd, Sr, Pb isotopes and K–Ar ages of basaltic rocks in Longhai and Mingxi, Fujian Province. Acta Petrologica Sinica 8, 324–331 (in Chinese with English abstract).

Chu, X.L., Li, X.L., Xu, J.H., Liu, J.M., 1999. Patterns of platinum-group elements in mantle peridotite, granulite xenoliths and basalt in Hannuoba. Chinese Science Bulletin 44, 859–863 (in Chinese).

Chung, S.-L., Cheng, H., Jahn, B.-M., O'Reilly, S.Y., Zhu, B., 1997. Major and trace element, and Sr–Nd isotope constraints on the origin of Paleogene volcanism in South China prior to the South China Sea opening. Lithos 40, 203–220.

Chung, S.-L., Sun, S.-S., Tu, K., Chen, C.-H., Lee, C.-Y., 1994. Late Cenozoic basaltic volcanism around the Taiwan Strait, SE China: product of lithosphere–asthenosphere interaction during continental extension. Chemical Geology 112, 1–20.

Craig, J.R., Scott, S.D., 1974. Sulfide phase equilibria. In: Ribbe, P.H. (Ed.), Sulfide Mineralogy. Mineralogical Society of America, pp. CS1–110.

Dale, C., Luguet, A., Macpherson, C., Pearson, D., Hickey-Vargas, R., 2008. Extreme platinum-group element fractionation and variable Os isotope compositions in Philippine Sea Plate basalts: tracing mantle source heterogeneity. Chemical Geology 248, 213–238.

Fan, Q., Hooper, P.R., 1991. The Cenozoic basaltic rocks of eastern China: petrology and chemical composition. Journal of Petrology 32, 765–810.

Fleet, M.E., Stone, W.E., Crocket, J.H., 1991. Partitioning of palladium, iridium, and platinum between sulfide liquid and basalt melt: effects of melt composition, concentration, and oxygen fugacity. Geochimica et Cosmochimica Acta 55, 2545–2554.

Govindaraju, K., 1994. Compilation of working values and sample description for 383 geostandards. Geostandards Newsletter 18, 1–158.

Green, N.L., 2006. Influence of slab thermal structure on basalt source regions and melting conditions: REE and HFSE constraints from the Garibaldi volcanic belt, northern Cascadia subduction system. Lithos 87, 23–49.

Greenough, J.D., Fryer, B.J., 1990. Distribution of gold, palladium, platinum, rhodium, ruthenium and iridium in Leg 115 Hotspot basalts: implication for magmatic processes. In: Duncan, R.A., Backman, J., Peterson, L.C. (Eds.), Proceedings of the Ocean Drilling Program, Scientific Results, pp. 71–84.

Greenough, J.D., Owen, J.V., 1992. Platinum-group element geochemistry of continental tholeiites—analysis of the Long-Range Dyke Swarm, Newfoundland, Canada. Chemical Geology 98, 203–219.

Hamlyn, P.R., Keays, R.R., 1986. Sulfur saturation and second-stage melts; application to the Bushveld platinum metal deposits. Economic Geology 81, 1431–1445.

Han, J.W., Xiong, X.L., Zhu, Z.Y., 2009. Geochemistry of Late-Cenozoic basalts from Leigiong area: the origin of EM2 and the contribution from sub-continental lithosphere mantle. Acta Petrologica Sinica 25, 3208–3220 (in Chinese with English abstract).

Hart, S.R., Dunn, T., 1993. Experimental cpx/melt partitioning of 24 trace elements. Contributions to Mineralogy and Petrology 113, 1–8.

Ho, K.-S., Chen, J.-C., Lo, C.-H., Zhao, H.-L., 2003. ^{40}Ar–^{39}Ar dating and geochemical characteristics of late Cenozoic basaltic rocks from the Zhejiang–Fujian region, SE China: eruption ages, magma evolution and petrogenesis. Chemical Geology 197, 287–318.

Huang, X.-L., Niu, Y., Xu, Y.-G., Ma, J.-L., Qiu, H.-N., Zhong, J.-W., 2013a. Geochronology and geochemistry of Cenozoic basalts from eastern Guangdong, SE China: constraints on the lithosphere evolution beneath the northern margin of the South China Sea. Contributions to Mineralogy and Petrology 165, 437–455.

Huang, X.-W., Zhou, M.-F., Wang, C.Y., Robinson, P.T., Zhao, J.-H., Qi, L., 2013b. Chalcophile element constraints on magma differentiation of Quaternary volcanoes in Tengchong, SW China. Journal of Asian Earth Sciences 76, 1–11.

Irvine, G.J., Pearson, D.G., Kjarsgaard, B.A., Carlson, R.W., Kopylova, M.G., Dreibus, G., 2003. A Re–Os isotope and PGE study of kimberlite-derived peridotite xenoliths from Somerset Island and a comparison to the Slave and Kaapvaal cratons. Lithos 71, 461–488.

Irving, A.J., Frey, F.A., 1978. Distribution of trace elements between garnet megacrysts and host volcanic liquids of kimberlitic to rhyolitic composition. Geochimica et Cosmochimica Acta 42, 771–787.

Jaques, A., Green, D., 1980. Anhydrous melting of peridotite at 0–15 kb pressure and the genesis of tholeiitic basalts. Contributions to Mineralogy and Petrology 73, 287–310.

Juang, W.S., Chen, J.C., 1992. Geochronology and geochemistry of Penghu basalts, Taiwan Strait and their tectonic significance. Journal of Southeast Asian Earth Sciences 7, 185–193.

Juang, W.-S., Chen, J.-C., 1999. The nature and origin of Penghu basalts: a review. Bulletin Central Geological Survey 12, 147–200.

Keays, R.R., 1995. The role of komatiitic and picritic magmatism and S-saturation in the formation of ore deposits. Lithos 34, 1–18.

Kelemen, P.B., Joyce, D.B., Webster, J.D., Holloway, J.R., 1990. Reaction between ultramafic rock and fractionating basaltic magma II. Experimental investigation of reaction between olivine Tholeiite and harzburgite at 1150–1050 °C and 5 kb. Journal of Petrology 31, 99–134.

Klemme, S., Günther, D., Hametner, K., Prowatke, S., Zack, T., 2006. The partitioning of trace elements between ilmenite, ulvöspinel, armalcolite and silicate melts with implications for the early differentiation of the Moon. Chemical Geology 234, 251–263.

Klock, W., Palme, H., 1988. Partitioning of siderophile and chalcophile elements between sulfide, olivine, and glass in a naturally reduced basalt from Disko Island, Greenland. In: Ryder, G. (Ed.), Proceedings of Lunar and Planetary Science Conference. Pergamon, New York, pp. 471–483.

Lightfoot, P.C., Keays, R.R., 2005. Siderophile and chalcophile metal variations in flood basalts from the Siberian Trap, Noril'sk Region: implications for the origin of the Ni–Cu–PGE sulfide ores. Economic Geology 100, 439–462.

Liu, R.X., Chen, W.J., Sun, J.Z., Li, D.M., 1992. The K–Ar age and tectonic environment of Cenozoic volcanic rocks in China (in Chinese with English abstract). The Age and Geochemistry of Cenozoic Volcanic Rock in China. Seismology Publ., Beijing, pp. 1–43.

Liu, Z.C., Wu, F.Y., Chu, Z.Y., Xu, X.S., 2010. Isotopic compositions of the peridotitic xenoliths from the Nushan area, Anhui Province: constraints on the age of subcontinental lithospheric mantle beneath the East China. Acta Petrologica Sinica 26, 1217–1240 (in Chinese with English abstract).

Luguet, A., Jaques, A.L., Pearson, D.G., Smith, C.B., Bulanova, G.P., Roffey, S.L., Rayner, M.J., Lorand, J.P., 2009. An integrated petrological, geochemical and Re–Os isotope study of peridotite xenoliths from the Argyle lamproite, Western Australia and implications for cratonic diamond occurrences. Lithos 112, 1096–1108.

Maier, W.D., Barnes, S.J., 2004. Pt/Pd and Pd/Ir ratios in mantle-derived magmas: a possible role for mantle metasomatism. South African Journal of Geology 107, 333–340.

McKenzie, D.P., O'Nions, R.K., 1991. Partial melt distributions from inversion of rare earth element concentrations. Journal of Petrology 32, 1021–1991.

McKenzie, D.P., O'Nions, R.K., 1995. The source regions of ocean island basalts. Journal of Petrology 36, 133–159.

Meisel, T., Moser, J., 2004. Reference materials for geochemical PGE analysis: new analytical data for Ru, Rh, Pd, Os, Ir, Pt and Re by isotope dilution ICP-MS in 11 geological reference materials. Chemical Geology 208, 319–338.

Momme, P., Óskarsson, N., Keays, R.R., 2003. Platinum-group elements in the Icelandic rift system: melting processes and mantle sources beneath Iceland. Chemical Geology 196, 209–234.

Mungall, J.E., Brenan, J.M., 2014. Partitioning of platinum-group elements and Au between sulfide liquid and basalt and the origins of mantle–crust fractionation of the chalcophile elements. Geochimica et Cosmochimica Acta 125, 265–289.

Naldrett, A.J., 2004. Magmatic Sulfide Deposits: Geology, Geochemistry and Exploration. Springer, New York.

Nanni, U., Pubellier, M., Chan, L.S., Sewell, R.J., 2017. Rifting and reactivation of a Cretaceous structural belt at the northern margin of the South China Sea. Journal of Asian Earth Sciences http://dx.doi.org/10.1016/j.jseaes.2017.01.008.

Orberger, B., Xu, Y., Reeves, S.J., 1998. Platinum group elements in mantle xenoliths from eastern China. Tectonophysics 296, 87–101.

Peach, C.L., Mathez, E.A., Keays, R.R., Reeves, S.J., 1994. Experimentally determined sulfide melt–silicate melt partition coefficients for iridium and palladium. Chemical Geology 117, 361–377.

Philipp, H., Eckhardt, J.D., Puchelt, H., 2001. Platinum-group elements (PGE) in basalts of the seaward-dipping reflector sequence, SE Greenland Coast. Journal of Petrology 42, 407–432.

Puchtel, I.S., Humayun, M., 2001. Platinum group element fractionation in a komatiitic basalt lava lake. Geochimica et Cosmochimica Acta 65, 2979–2993.

Qi, L., Gao, J., Huang, X., Hu, J., Zhou, M.-F., Zhong, H., 2011. An improved digestion technique for determination of platinum group elements in geological samples. Journal of Analytical Atomic Spectrometry 26, 1900–1904.

Qi, L., Hu, J., Gregoire, D.C., 2000. Determination of trace elements in granites by inductively coupled plasma mass spectrometry. Talanta 51, 507–513.

Qi, Q., Taylor, L.A., Zhou, X., 1994. Geochemistry and petrogenesis of three series of Cenozoic basalts from southeastern China. International Geology Review 36, 435–451.

Qi, L., Wang, C.Y., Zhou, M.-F., 2008. Controls on the PGE distribution of Permian Emeishan alkaline and peralkaline volcanic rocks in Longzhoushan, Sichuan Province, SW China. Lithos 106, 222–236.

Qi, L., Zhou, M.F., 2008. Platinum-group elemental and Sr–Nd–Os isotopic geochemistry of Permian Emeishan flood basalts in Guizhou Province, SW China. Chemical Geology 248, 83–103.

Qi, L., Zhou, M.-F., Wang, C.Y., 2004. Determination of low concentrations of platinum group elements in geological samples by ID-ICP-MS. Journal of Analytical Atomic Spectrometry 19, 1335–1339.

Rehkämper, M., Halliday, A.N., Fitton, J.G., Lee, D.C., Wieneke, M., Arndt, N.T., 1999. Ir, Ru, Pt, and Pd in basalts and komatiites: new constraints for the geochemical behavior of the platinum-group elements in the mantle. Geochimica et Cosmochimica Acta 63, 3915–3934.

Righter, K., Campbell, A.J., Humayun, M., Hervig, R.L., 2004. Partitioning of Ru, Rh, Pd, Re, Ir, and Au between Cr-bearing spinel, olivine, pyroxene and silicate melts. Geochimica et Cosmochimica Acta 68, 867–880.
Salters, V.J.M., Andreas, S., 2004. Composition of the depleted mantle. Geochemistry, Geophysics, Geosystems 5, 469–484.
Shaw, D.M., 1970. Trace element fractionation during anatexis. Geochimica et Cosmochimica Acta 34, 237–243.
Sun, S.S., McDonough, W.F., 1989. Chemical and isotopic systematics of oceanic basalts: implications for mantle composition and processes. Geological Society of London, Special Publication 42, 313–345.
Tapponnier, P., Peltzer, G., Le Dain, A.Y., Armijo, R., Cobbold, P., 1982. Propagating extrusion tectonics in Asia: new insights from simple experiments with plasticine. Geology 10, 611–616.
Tatsumoto, M., Basu, A.R., Huang, W., Wang, J., Xie, G., 1992. Sr, Nd, and Pb isotopes of ultramafic xenoliths in volcanic rocks of Eastern China: enriched components EMI and EMII in subcontinental lithosphere. Earth and Planetary Science Letters 113, 107–128.
Tu, K., Flower, M.F.J., Carlson, R.W., Xie, G.H., Chen, C.Y., Zhang, M., 1992. Magmatism in the South China Basin: 1. Isotopic and trace element evidence for an endogenous Dupal mantle component. Chemical Geology 97, 47–63.
Tu, K., Flower, M.F., Carlson, R.W., Zhang, M., Xie, G., 1991. Sr, Nd, and Pb isotopic compositions of Hainan basalts (south China): implications for a subcontinental lithosphere Dupal source. Geology 19, 567–569.
Wang, K.-L., Chung, S.-L., Lo, Y.-M., Lo, C.-H., Yang, H.-J., Shinjo, R., Lee, T.-Y., Wu, J.-C., Huang, S.-T., 2012. Age and geochemical characteristics of Paleogene basalts drilled from western Taiwan: records of initial rifting at the southeastern Eurasian continental margin. Lithos 155, 426–441.
Wang, K.L., O'Reilly, S.Y., Griffin, W.L., Pearson, N.J., Zhang, M., 2009. Sulfides in mantle peridotites from Penghu Islands, Taiwan: melt percolation, PGE fractionation, and the lithospheric evolution of the South China block. Geochimica et Cosmochimica Acta 73, 4531–4557.
Wang, C.Y., Zhou, M.F., Qi, L., 2007. Permian flood basalts and mafic intrusions in the Jinping (SW China)–Song Da (northern Vietnam) district: mantle sources, crustal contamination and sulfide segregation. Chemical Geology 243, 317–343.
Wang, C.Y., Zhou, M.F., Qi, L., 2011. Chalcophile element geochemistry and petrogenesis of high-Ti and low-Ti magmas in the Permian Emeishan large igneous province, SW China. Contributions to Mineralogy and Petrology 161, 237–254.
Xu, Y.G., Orberger, B., Reeves, S.J., 1998. Fractionation of platinum group elements in upper mantle: evidence from peridotite xenoliths from Wangqing. Science in China Series D-Earth Sciences 41, 354–361 (in Chinese with English abstract).
Xu, X., O'Reilly, S.Y., Griffin, W., Zhou, X., 2003. Enrichment of upper mantle peridotite: petrological, trace element and isotopic evidence in xenoliths from SE China. Chemical Geology 198, 163–188.
Xu, Y., Sun, M., Yan, W., Liu, Y., Huang, X., Chen, X., 2002. Xenolith evidence for polybaric melting and stratification of the upper mantle beneath South China. Journal of Asian Earth Sciences 20, 937–954.
Xu, Y., Wei, J., Qiu, H., Zhang, H., Huang, X., 2012. Opening and evolution of the South China Sea constrained by studies on volcanic rocks: preliminary results and a research design. Chinese Science Bulletin 57, 3150–3164.
Yang, A.Y., Zhao, T.P., Qi, L., Yang, S.H., Zhou, M.F., 2011. Chalcophile elemental constraints on sulfide-saturated fractionation of Cenozoic basalts and andesites in SE China. Lithos 127, 323–335.
Yoder, H.S., Tilley, C.E., 1962. Origin of basalt magmas: an experimental study of natural and synthetic rock systems. Journal of Petrology 3, 342–532.
Yu, J.-H., O'Reilly, S.Y., Zhang, M., Griffin, W.L., Xu, X., 2006. Roles of melting and metasomatism in the formation of the lithospheric mantle beneath the Leizhou Peninsula, South China. Journal of Petrology 47, 355–383.
Yurimoto, H., Ohtani, E., 1992. Element partitioning between majorite and liquid: a secondary ion mass spectrometric study. Geophysical Research Letters 19, 17–20.
Zeng, G., Huang, X.-W., Zhou, M.-F., Chen, L.-H., Xu, X.-S., 2016. Using chalcophile elements to constrain crustal contamination and xenolith–magma interaction in Cenozoic basalts of Eastern China. Lithos 258-259, 163–172.
Zheng, J., Sun, M., Zhou, M.-F., Robinson, P., 2005. Trace elemental and PGE geochemical constraints of Mesozoic and Cenozoic peridotitic xenoliths on lithospheric evolution of the North China Craton. Geochimica et Cosmochimica Acta 69, 3401–3418.
Zhou, X., Armstrong, R.L., 1982. Cenozoic volcanic rocks of eastern China—secular and geographic trends in chemistry and strontium isotopic composition. Earth and Planetary Science Letters 58, 301–329.
Zhou, X., Carlson, R., 1982. Isotopic Evidence for Temporal Variability of Mantle Characteristics Beneath the North China Fault Block. Carnegie Inst. Washington, Dep. Terr. Magn. Annu. Rep Vol. 81 p. 505.
Zhou, M.F., Sun, M., Keays, R.R., Kerrich, R.W., 1998. Controls on platinum-group elemental distributions of podiform chromitites: a case study of high-Cr and high-Al chromitites from Chinese orogenic belts. Geochimica et Cosmochimica Acta 62, 677–688.
Zhou, H., Xiao, L., Dong, Y., Wang, C., Wang, F., Ni, P., 2009. Geochemical and geochronological study of the Sanshui basin bimodal volcanic rock suite, China: implications for basin dynamics in southeastern China. Journal of Asian Earth Sciences 34, 178–189.
Zou, H., Zindler, A., Xu, X., Qi, Q., 2000. Major, trace element, and Nd, Sr and Pb isotope studies of Cenozoic basalts in SE China: mantle sources, regional variations, and tectonic significance. Chemical Geology 171, 33–47.